The Astrophysical Journal, 549:L147–L150, 2001 March 1

X-RAY VELOCIMETRY OF SOLAR WIND ION IMPACT ON COMETS

P. Beiersdorfer,[1] C. M. Lisse,[2] R. E. Olson,[3] G. V. Brown,[1] and H. Chen[1]
Received 2000 November 6; accepted 2001 January 26; published 2001 February 26

ABSTRACT

Laboratory measurements of the interaction of low-energy, bare, and hydrogen-like ions with neutral gases are presented. The measurements demonstrate that charge-exchange–induced cometary K-shell X-ray spectra represent rich spectral diagnostics for determining the speed of the solar wind and the collision dynamics within the coma. We show that the K-shell spectrum observed from low-energy ion-neutral collisions ($\leq$ 50 km s^{-1}) has a distinct high-energy component that is suppressed in high-energy collisions ($\geq$800 km s^{-1}). As a result, the hardness ratio of the K-shell spectrum increases by as much as a factor of 4 as the ions decelerate in the coma. The change in spectral shape can be observed even with low-resolution energy dispersive solid-state detectors, opening the possibility of spatial imaging of the solar wind heavy-ion velocity profile in the coma. Our results clearly show that energy-dependent data are needed to fully describe charge-exchange–induced X-ray production in the heliosphere.

Subject headings: atomic data — atomic processes — comets: general — X-rays: general

1. INTRODUCTION

Following the surprise discovery of X-ray emission from comet Hyakutake by *ROSAT* (Lisse et al. 1996; Häberli et al. 1997; Wegmann et al. 1998), numerous comets have been shown to emit X-rays (Dennerl, Englhauser, & Trümper 1997; Mumma, Krasnopolsky, & Abbott 1997; Lisse et al. 1999a), and comets are now classified as X-ray sources in the solar system, achieving fluxes as high as 10^{25} photons s^{-1} (Mumma et al. 1997; Krasnopolsky et al. 1997). While many models have been proposed to explain the observations, one appears to be the most probable, i.e., charge transfer between solar wind heavy ions and neutral gases in the coma (Krasnopolsky 1997; Cravens 1997; Wegmann et al. 1998; Lisse et al. 1999b).

The interaction between the solar wind and comets provides a potentially very powerful means to someday monitor space weather in situ by providing such parameters as composition of the solar wind as well as real-time observation of solar activity, e.g., occurrences of coronal mass ejections and the evolution of solar wind sector boundaries (Neugebauer et al. 2000), without the need for heliospheric spacecraft. Comets could be used as probes throughout much of the year given that more than three bright comets with appreciable X-ray emission (i.e., $V < 12$) enter the inner solar system each year. Moreover, comets sample regions of space that are out of reach of current solar wind monitors, e.g., large heliocentric distances and latitude. Understanding the details of the emission produced in the interaction of the solar wind and comets is a prerequisite for such an application.

Heavy ions in the solar wind are produced with velocities up to 800 km s^{-1} or, equivalently, energies of 3 keV amu^{-1} (McComas et al. 1998). As a result, predictions of the X-ray emission reported to date have focused on multi-keV ion-neutral collisions. At very high collision energies it is appropriate to incorporate assumptions of statistical populations of the excited states in predictions of the X-ray emission; i.e., each angular momentum state may be assumed to be uniformly populated weighted by the degeneracy of the state. This is a valid assumption for high-energy ($\geq$10 keV amu^{-1}) collisions studied with heavy-ion accelerators and beam-heated magnetic fusion devices. Such an assumption was used by Häberli et al. (1997) in one of the first models to predict the shape of the X-ray emission from comets. At a collision energy of 3 keV amu^{-1} (the maximum solar wind ion energy), this assumption is only marginally valid. Already at these relatively high energies excited levels are populated in a nonstatistical way (Dijkkamp et al. 1985; Burgdörfer, Morgenstern, & Niehaus 1986). As the ions penetrate the coma, they slow down. The collision energy is typically a few hundred eV amu^{-1} just outside the bow shock, and it may be 50 eV amu^{-1} or less in the inner region (Krasnopolsky 1997). Recent imaging of the X-ray emission morphology of 2P/Encke 1997 by Lisse et al. (1999b) has shown that a substantial fraction (up to 50%) of the observed X-ray emission may emanate from the region inside the bow shock and near the nucleus where the collision energy is 1–2 orders of magnitude lower. At such low energies any statistical assumptions break down completely, and the X-ray emission from these regions of low-energy ion-neutral collisions is not described by the present models.

Very little theoretical or experimental data are available that describe charge-exchange–induced X-ray emission at low collision energies. In fact, even the very detailed modeling calculations of the X-rays produced by charge-exchange collisions recently presented by Kharchenko & Dalgarno (2000) do not take into account the possible variability of the X-ray emission with collision energy. At the same time, experiments of charge-exchange–induced X-ray emission have focused only on the high end of the collision energies (Greenwood et al. 2000).

To investigate the low-energy behavior of charge-exchange collisions, we used the Livermore electron beam ion trap EBIT-II. The ion-neutral collision energy in this device is below 20 eV amu^{-1} (Beiersdorfer et al. 1996a). Our measurements focused on the K-shell X-ray emission from the charge-transfer reaction $O^{8+} + CO_2$ and $O^{7+} + CO_2$, as well as Ne^{10+} + Ne and Ne^{9+} + Ne. Oxygen and neon ions are a constituent of the solar wind, and these measurements are representative of the processes affecting all K-shell solar wind ions (C, N, O, Ne) at low collision energy.

[1] Department of Physics, Lawrence Livermore National Laboratory, Livermore, CA 94551.
[2] Space Telescope Science Institute, Baltimore, MD 21218.
[3] Department of Physics, University of Missouri–Rolla, Rolla, MO 65401.

2. EXPERIMENTAL

Electron beam ion traps were described in detail by Levine et al. (1988) and Marrs, Beiersdorfer, & Schneider (1994). Our EBIT-II device has been optimized for laboratory astrophysics measurements over the past decade and includes a suite of spectroscopic diagnostics that allow us to monitor and investigate the relevant plasma parameters and atomic processes (Beiersdorfer et al. 2000a,[4] 2000b).

For the present measurements, the oxygen and neon ions were produced in situ by collisional ionization in the interaction with an energetic electron beam. About 10^7 ions were produced. The beam was then turned off, and the trap operated in the so-called magnetic mode (Beiersdorfer et al. 1996b). In this mode, the ions were confined radially by a 3 T axial magnetic field and longitudinally by a 200 V potential on the top and bottom electrodes. X-rays produced in the charge-transfer collisions involving the trapped neon ions and ambient neutral atoms were monitored with a windowless, high-purity Ge detector with a resolution $\Delta E \approx 140$–180 eV at the 500–1400 eV energy range of interest. The collision energy was estimated from the trapping conditions to be about 15 ± 5 eV amu^{-1} for oxygen and 9 ± 4 eV amu^{-1} for neon.

The measured X-ray emission from neon is shown in Figure 1. By proper choice of the electron beam energy, we produced only Ne^{9+} ions or a mixture of Ne^{9+} and Ne^{10+} ions. The latter resulted in X-ray emission that contained K-shell X-rays from both ion species undergoing charge-transfer reactions. The pure X-ray emission for Ne^{10+} collisions was readily determined by appropriate subtraction of the Ne^{9+} contribution. A similar procedure was employed for oxygen. However, because oxygen emits K-shell photons at substantially lower energies than neon, which can only barely be resolved with our Ge detector, our measurements are of much lower quality.

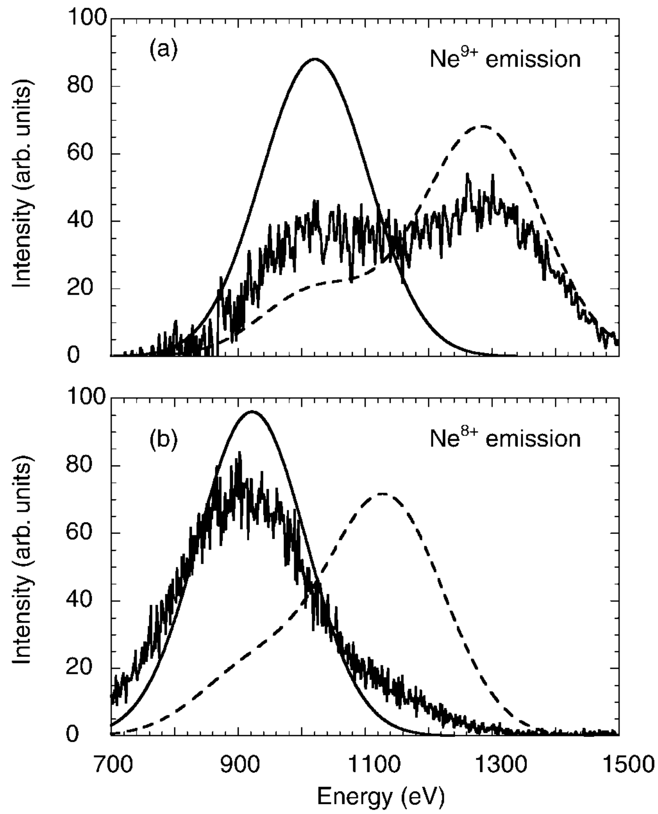

FIG. 1.—Laboratory observation of the K-shell X-ray emission from charge-exchange reactions: (*a*) $Ne^{10+} + Ne \rightarrow Ne^{9+} + Ne^{+}$, (*b*) $Ne^{9+} + Ne \rightarrow Ne^{8+} + Ne^{+}$. The solid curves represent predictions using the model by Häberli et al. (1997); the dashed curves represent predictions using the model by Wegmann et al. (1998).

3. DISCUSSION

Constrained by the principle of energy conservation, charge exchange populates levels of bare neon with principal quantum number $n_c = 5$ or $n_c = 6$ depending on the ionization potential of the neutral species (Olson 1981). In high-energy collisions, angular momentum states are populated statistically by weight of the state's degeneracy. The angular momentum state $l_c = n_c - 1$, which has the highest statistical weight, has the highest probability of occupation. Selection rules favor $\Delta l = \pm 1$ transitions, and the excited electron predominantly cascades via $\Delta n = 1$ transitions. An X-ray is given off only in the last step from $n = 2$ to $n = 1$. Direct decay from $n = n_c$ to $n = 1$ has only a small likelihood. This likelihood can be approximated by the fractional statistical weight of the $n = n_c$, $l = 1$ state, which in the high-energy limit is the ratio of the statistical weight of the $l = 1$ state ($=3$) to the sum of the statistical weights of all other angular momentum states ($= n_c^2 - 3$). For neon the fraction is, thus, less than 15%. As mentioned before, Häberli et al. (1997) used this scheme to build their cometary X-ray emission model, including only the dominant $n = 2$ to $n = 1$ K-shell decays. Based on their model, the highest energy X-ray produced in the reaction $Ne^{10+} + Ne$ would be Lyα emission at 1022 eV. Looking at our measurement shown in Figure 1*a*, this is clearly not the case. X-ray emission extending above 1300 eV is observed, with the total flux of this high-energy emission larger than the flux in the $n = 2$ to $n = 1$ emission.

The high-energy emission is produced in the direct decay of the $n_c = 5, 6$ electron to a K-shell vacancy (or via one or two steps to $n \geq 3$ levels). The selection rules dictate that only electrons with $l = 1$ angular momentum (*p* state) can undergo such a transition. As a result, the prominence of the observed high-energy emission implies that electrons are captured with angular momentum values that peak near $l = 1$. This contradicts the assumption of statistical population of the angular momentum states and proves that low-energy collisions produce X-ray emission very different from the patterns observed in high-energy collisions. Wegmann et al. (1998) developed a cometary X-ray model that includes contributions from high-*n* emission. Their model resulted in better agreement with cometary spectra. However, their model of high-*n* emission is based on unphysical radiative branching ratios by assuming all levels between $n = 2$ and $n = n_c$ radiate in equal amounts. Their model also does not reproduce the laboratory observations (cf. Fig. 1).

At first thought, one would expect the X-ray emission pattern from collisions involving Ne^{9+} to match that involving Ne^{10+}. Looking at the measurement in Figure 1*b* we see this is not at all the case. As before, the electron is captured into $n_c = 5, 6$ with an angular momentum near $l = 1$. However, the presence of an unpaired electron in the K shell changes the radiative decay paths drastically. The fact that only about 10%

[4] See also http://heasarc.gsfc.nasa.gov/docs/heasarc/atomic.

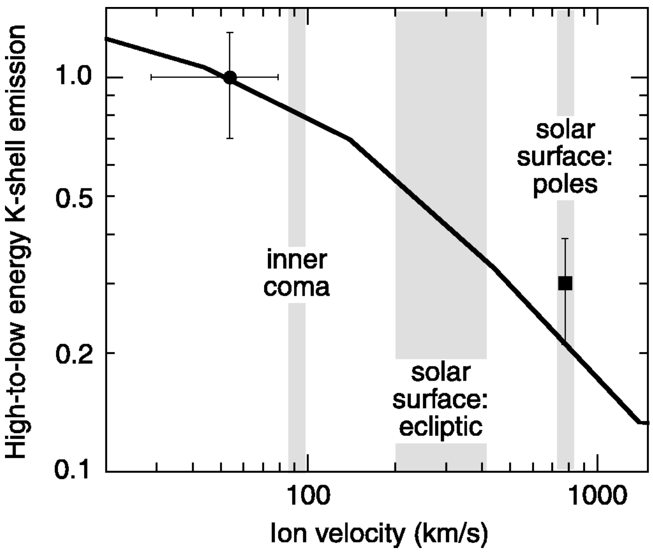

FIG. 2.—Hardness ratio of the K-shell X-ray emission following charge-exchange reaction $O^{8+} + A \rightarrow O^{7+} + A^{+}$ as a function of the relative ion velocity. The K-shell hardness ratio is defined as the strength of the $n = 3, 4, \ldots, n_c \rightarrow n = 1$ emission relative to the $n = 2 \rightarrow n = 1$ emission. The solid curve was calculated using the CTMC technique. The value measured in the present experiment is shown as a solid circle. The value inferred from the results of Greenwood et al. (2000) is shown as a solid square. Hatched areas indicate ion velocities in the high solar latitude, the ecliptic, and behind the bow shock.

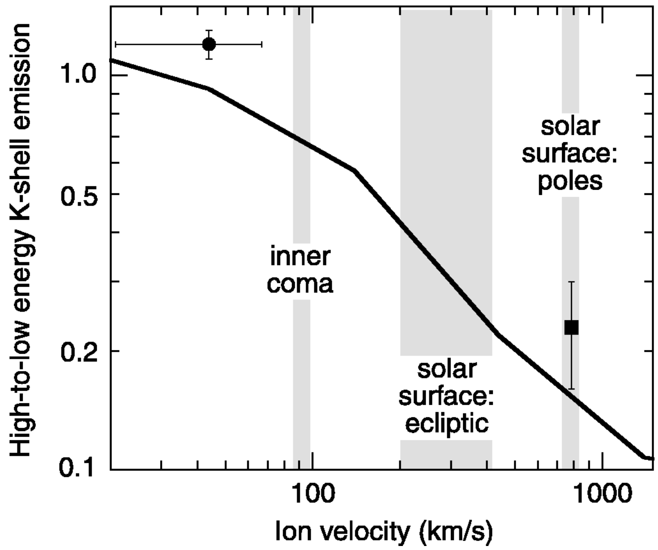

FIG. 3.—Hardness ratio of the K-shell X-ray emission following charge-exchange reaction $Ne^{10+} + A \rightarrow Ne^{9+} + A^{+}$ as a function of the relative ion velocity. The conventions are the same as in Fig. 2.

of the observed X-ray emission is from $n \geq 3$ to $n = 1$ decay proves that capture produces a triplet level ($1sn_c p\ ^3P_1$) in the helium-like neon ion. In fact, statistical considerations require that capture into triplet states are favored 3 : 1 over capture into singlet states. The $1sn_c p\ ^3P_1$ triplet level is spin-forbidden to decay to the $1s^2\ ^1S_0$ helium-like ground state. The upper level decays instead to the $1s2s\ ^3S_1$ level. This level is also spin-forbidden to decay to the ground state. But given no other radiative decay path, it will do so in a low-density, collisionless environment, as in cometary comae or our trap, via the emission of a K-shell X-ray. Again, this decay scheme is very different from that expected in high-energy collisions. A comparison with the Häberli et al. (1997) model shows reasonable agreement, albeit for fortuitous reasons. No agreement is found with the Wegmann et al. (1998) model.

A more detailed cometary X-ray emission model was recently presented by Kharchenko & Dalgarno (2000). Unlike other cometary X-ray models, Kharchenko & Dalgarno included full accounting of principal and angular momentum quantum numbers and their effect on radiative cascades leading to X-ray emission. Their results agree qualitatively with our observations for both the hydrogenic and helium-like emission. For example, they predict that the spectral emission of helium-like ions differs significantly from that of hydrogenic ions because of the role played by the electron spin coupling. Like the authors of the other models, however, they do not take into account the effect of variations of the collision energy and do not predict the changes of the X-ray emission spectrum as a function of collision energy uncovered by our measurements.

The fact that the spectral emission does not follow simple statistical rules but instead depends on the collision energies in the range of interest to comets means that cometary X-ray spectra provide information beyond solar activity and solar wind composition. The ratio of high to low energy K-shell line intensity provides a powerful diagnostic marker of the collision dynamics inside and outside the bow shock. As the ions pass through the bow shock region and slow down, the center-of-mass collision energy decreases and the population of low angular momentum states becomes increasingly more probable. This results in an increase in the high-energy emission from a given species and thus in the hardness of the cometary spectrum.

The increase in the high-energy emission is illustrated in Figures 2 and 3, where we plot the calculated ratio of the X-ray emission from $n \geq 3$ relative to the $n = 2$ K-shell emission, i.e., the hardness ratio, as a function of the collision velocity. The curves are calculated using the classical trajectory Monte Carlo (CTMC) technique (Olson, Pascale, & Hoekstra 1992) for the reactions $O^{8+} + A \rightarrow O^{7+} + A^{+}$ (Fig. 2) and $Ne^{10+} + A \rightarrow Ne^{9+} + A^{+}$ (Fig. 3). On the scale shown, the results are insensitive to the nature of gas A. These calculations not only provide cross sections of capture into specific n shells but also give the detailed angular momentum distribution. In order to deduce the actual X-ray emission from the CTMC capture cross sections, we assumed a hydrogenic radiative cascade model.

For comparison, Figures 2 and 3 show our experimental data for the X-ray hardness ratio from O^{7+} and Ne^{9+}, respectively. These agree well with our CTMC calculations, especially the oxygen value. We note that this agreement is much better than that for higher Z ions at similarly low collision velocities, which we reported recently (Beiersdorfer et al. 2000c). The figures also show the data reported by Greenwood et al. (2000). Their values were measured at the high end of the solar wind velocities. Although somewhat larger than our CTMC results, they fit well with the overall scaling of the X-ray hardness ratio as a function of collision velocity.

Figures 2 and 3 show that there is an increase of about a factor of 3–4 in the hardness ratio as the solar wind ions pass through the bow shock region and slow down as a result of pickup and mass loading of slow-moving ions from the comet.

The ratio, thus, represents a powerful remote diagnostic tool for the physical conditions in the interaction region between solar wind and cometary coma from which the degree of ion deceleration and mass pickup can potentially be inferred.

Moreover, solar wind velocity varies strongly with heliographic latitude. We predict based on our results that the hardness of the cometary spectra varies with the physical position of the comet with respect to the ecliptic. In fact, there is a factor of 2 difference in the hardness ratio depending on whether the ions emanate from the solar equator, where solar wind velocities are about 200 km s^{-1}, or from the solar poles, where the velocities are about 800 km s^{-1}. The X-ray emission thus can be used as a monitor of the solar wind speed and composition throughout the heliosphere. Moreover, the hardness ratio may be a diagnostic for discerning the soft X-ray background from the heliopause and, in turn, may play a role in determining mass-loss rates of nearby stars (Cravens 2000; Wargelin & Drake 2001).

This work was performed under the auspices of the Department of Energy by the University of California Lawrence Livermore National Laboratory under contract W-7405-ENG-48 and supported in part by the Chemical Sciences, Geosciences and Biosciences Division of the Office of Basic Energy Sciences, Office of Science, US Department of Energy. C. M. L.'s research was supported in part by NASA's Planetary Astronomy Program grant NAGW-188 and by observing grants NAG5-6141 and NAG-6155.

REFERENCES

Beiersdorfer, P., Brown, G. V., Chen, H., Gu, M.-F., Kahn, S. M., Lepson, J. K., Savin, D. W., & Utter, S. B. 2000a, in Atomic Data Needs for X-Ray Astronomy, ed. M. A. Bautista, T. R. Kallman, & A. K. Pradhan (NASA/CP-2000-209968; Greenbelt: NASA GSFC), 103

Beiersdorfer, P., et al. 2000b, Rev. Mexicana Astron. Astrofis., 9, 123

———. 2000c, Phys. Rev. Lett., 85, 5090

Beiersdorfer, P., Osterheld, A. L., Decaux, V., & Widmann, K. 1996a, Phys. Rev. Lett., 77, 5353

Beiersdorfer, P., Schweikhard, L., Crespo López-Urrutia, J., & Widmann, K. 1996b, Rev. Sci. Instrum., 67, 3818

Burgdörfer, J., Morgenstern, R., & Niehaus, A. 1986, J. Phys. B, 19, L503

Cravens, T. E. 1997, Geophys. Res. Lett., 24, 105

———. 2000, ApJ, 532, L153

Dennerl, K., Englhauser, J., & Trümper, J. 1997, Science, 277, 1625

Dijkkamp, D., Gordeev, Yu. S., Brazuk, A., Drentje, A. G., & de Heer, F. J. 1985, J. Phys. B, 18, 737

Greenwood, J. B., Williams, I. D., Smith, S. J., & Chutjian, A. 2000, ApJ, 533, L175

Häberli, R. M., Gombosi, T. I., De Zeeuw, D. L., Combi, M. R., & Powell, K. G. 1997, Science, 276, 939

Kharchenko, V., & Dalgarno, A. 2000, J. Geophys. Res., 105, 18351

Krasnopolsky, V. A. 1997, Icarus, 128, 368

Krasnopolsky, V. A., Mumma, M. J., Abbott, M., Flynn, B. C., Meech, K. J., Yeomans, D. K., Feldmann, P. D., & Cosmovici, C. B. 1997, Science, 277, 1488

Levine, M. A., Marrs, R. E., Henderson, J. R., Knapp, D. A., & Schneider, M. B. 1988, Phys. Scr., T22, 157

Lisse, C. M., et al. 1996, Science, 274, 205

———. 1999a, Earth Moon Planets, 77, 283

———. 1999b, Icarus, 141, 316

Marrs, R. E., Beiersdorfer, P., & Schneider, D. 1994, Phys. Today, 47, 27

McComas, D. J., et al. 1998, Geophys. Res. Lett., 25, 1

Mumma, M. J., Krasnopolsky, V. A., & Abbott, M. J. 1997, ApJ, 491, L125

Neugebauer, M., Cravens, T. E., Lisse, C. M., Ipavich, F. M., von Steiger, R., Shah, P. D., & Armstrong, T. P. 2000, J. Geophys. Res., 105, 20949

Olson, R. E. 1981, Phys. Rev. A, 24, 1726

Olson, R. E., Pascale, J., & Hoekstra, R. 1992, J. Phys. B, 25, 4241

Wargelin, B. J., & Drake, J. J. 2001, ApJ, 546, L57

Wegmann, R., Schmidt, H. U., Lisse, C. M., Dennerl, K., & Englhauser, J. 1998, Planet. Space Sci., 46, 603